NAVAL POSTGRADUATE SCHOOL

MONTEREY, CALIFORNIA

THESIS

SYNOPTIC CONDITIONS CONTRIBUTING TO LIGHTNING EVENTS IN COASTAL CALIFORNIA

by

Kira B. Schlosberg

December 2018

Thesis Advisor: John M. Peters
Second Reader: Wendell A. Nuss

THIS PAGE INTENTIONALLY LEFT BLANK

REPORT DOCUMENTATION PAGE			*Form Approved OMB No. 0704-0188*

1. AGENCY USE ONLY *(Leave blank)*	**2. REPORT DATE** December 2018	**3. REPORT TYPE AND DATES COVERED** Master's thesis

4. TITLE AND SUBTITLE SYNOPTIC CONDITIONS CONTRIBUTING TO LIGHTNING EVENTS IN COASTAL CALIFORNIA	**5. FUNDING NUMBERS**
6. AUTHOR(S) Kira B. Schlosberg	
7. PERFORMING ORGANIZATION NAME(S) AND ADDRESS(ES) Naval Postgraduate School Monterey, CA 93943-5000	**8. PERFORMING ORGANIZATION REPORT NUMBER**
9. SPONSORING / MONITORING AGENCY NAME(S) AND ADDRESS(ES) N/A	**10. SPONSORING / MONITORING AGENCY REPORT NUMBER**

11. SUPPLEMENTARY NOTES The views expressed in this thesis are those of the author and do not reflect the official policy or position of the Department of Defense or the U.S. Government.

12a. DISTRIBUTION / AVAILABILITY STATEMENT Approved for public release. Distribution is unlimited.	**12b. DISTRIBUTION CODE** A

13. ABSTRACT (maximum 200 words)

Wildfires present an increased risk to the environment and population of California. In coastal regions of California, the presence of lightning is relatively uncommon compared to California as a whole. While lightning-triggered fires are less common than those started by other means, there is the potential to increase predictability of fires started by lightning by analyzing weather patterns. This study found that three primary synoptic patterns occur when cloud-to-ground lightning is observed in coastal California. Additionally, the study found atmospheric characteristics present during lightning events that forecasters should pay attention to in order to improve lightning forecasts. The study also found that lightning is triggered by primarily elevated convection during the summer months and surface-based convection during the remaining months of the year. By determining the general weather patterns that correspond with lightning strikes in coastal regions and informing forecasters of practical techniques to increase accuracy for lightning forecasts, first responders can be more aware of the potential risks of lightning-triggered fires during the dry months. This can lead to better fire response and an increase in preventative measures for both the environment and the California population.

14. SUBJECT TERMS lightning, convection, climate, California, coastal meteorology	**15. NUMBER OF PAGES** 49
	16. PRICE CODE

17. SECURITY CLASSIFICATION OF REPORT	**18. SECURITY CLASSIFICATION OF THIS PAGE**	**19. SECURITY CLASSIFICATION OF ABSTRACT**	**20. LIMITATION OF ABSTRACT**
Unclassified	Unclassified	Unclassified	UU

NSN 7540-01-280-5500 Standard Form 298 (Rev. 2-89) Prescribed by ANSI Std. 239-18

THIS PAGE INTENTIONALLY LEFT BLANK

Approved for public release. Distribution is unlimited.

SYNOPTIC CONDITIONS CONTRIBUTING TO LIGHTNING EVENTS IN COASTAL CALIFORNIA

Kira B. Schlosberg
Second Lieutenant, United States Air Force
BS, Air Force Academy, 2017

Submitted in partial fulfillment of the
requirements for the degree of

MASTER OF SCIENCE IN METEOROLOGY

from the

NAVAL POSTGRADUATE SCHOOL
December 2018

Approved by: John M. Peters
Advisor

Wendell A. Nuss
Second Reader

Wendell A. Nuss
Chair, Department of Meteorology

THIS PAGE INTENTIONALLY LEFT BLANK

ABSTRACT

Wildfires present an increased risk to the environment and population of California. In coastal regions of California, the presence of lightning is relatively uncommon compared to California as a whole. While lightning-triggered fires are less common than those started by other means, there is the potential to increase predictability of fires started by lightning by analyzing weather patterns. This study found that three primary synoptic patterns occur when cloud-to-ground lightning is observed in coastal California. Additionally, the study found atmospheric characteristics present during lightning events that forecasters should pay attention to in order to improve lightning forecasts. The study also found that lightning is triggered by primarily elevated convection during the summer months and surface-based convection during the remaining months of the year. By determining the general weather patterns that correspond with lightning strikes in coastal regions and informing forecasters of practical techniques to increase accuracy for lightning forecasts, first responders can be more aware of the potential risks of lightning-triggered fires during the dry months. This can lead to better fire response and an increase in preventative measures for both the environment and the California population.

THIS PAGE INTENTIONALLY LEFT BLANK

TABLE OF CONTENTS

THIS PAGE INTENTIONALLY LEFT BLANK

LIST OF FIGURES

LIST OF ACRONYMS AND ABBREVIATIONS

CAA	cold air advection
CAPE	convective available potential energy
GFS	Global Forecast System
NCEI	National Centers for Environmental Energy
NCEP	National Centers for Environmental Prediction
PC	principal component
PCA	principal component analysis
UCAR	University Corporation for Atmospheric Research

THIS PAGE INTENTIONALLY LEFT BLANK

ACKNOWLEDGMENTS

I wanted to take some time to thank all of those who contributed to getting me into and through the Basic Meteorology Program at NPS. Major Greg Strong, thank you for believing in me and getting me this position here at NPS, as well as for your mentorship and career advice. Thank you to all who advocated for the Basic Meteorology Program to be offered at NPS, Dr. Wendell Nuss, Colonel Sands, and anyone else who may have contributed to the program. I am extremely grateful for this unique opportunity. Thank you to Lt Col Jaramillo for teaching me valuable information that will help me down the road in my career, as well as for approving my numerous pass and leave requests.

To my Air Force cohort: I am forever grateful for your friendship and mentorship. Without all of you, life at NPS would not have been anywhere near as great as it was!

To all of my professors and instructors I have had the pleasure of learning from while at NPS, thank you for your wisdom and patience! To Dr. Wendell Nuss, thank you for taking on the Basic Meteorology Program here and facilitating the ability for me to pursue my master's degree. Without your help and advocacy, this degree would not have been possible. To Dr. John Peters, thank you for your help on this thesis. Without your guidance and support, this would not have come together in the short amount of time that we had to work with. I am grateful for all of your help!

Finally, to my family, thank you for setting me up with the skills necessary to be able to pursue my master's degree. And to Nate, thank you for always motivating, always loving me, and attempting to keep me sane over the past 1.5 years. I would not be here without you and your unconditional love and support!

THIS PAGE INTENTIONALLY LEFT BLANK

I. INTRODUCTION

Wildfires in California pose a major threat to the population and environment. The two primary sources of wildfires are lightning and humans, with lightning generating approximately 10% of the fires (CAL FIRE, 2009). While humans contribute more to the development of fires than lightning, fires have been present in California dating back thousands of years. Analysis of 16,000-year-old sediment from one of Yosemite's lakes indicated the presence of fire in the region, most likely due to lightning (Smith and Anderson 1992). A study mapping the location of fires requiring Forest Service action in California from 1911–1920 that were started by lightning, indicated that the concentration of lightning fires is more significant in the northern region of the state than inland regions, with the concentration decreasing towards the southern boundary of the state (Show and Kotok 1923). Although this study includes only lightning-based fires that required Forest Service action, it provides useful information on the general location trend of lightning-based fires in California.

In August 1987, the Stanislaus Complex Fire, started by dry lightning strikes, burned more than 600,000 acres in northern California (Duclos et al. 1989). Throughout the region most affected by the fire, a study was conducted in the emergency rooms to indicate the effect that fires and smoke have on public health. The study found that patients visiting with asthma, chronic obstructive pulmonary disease, sinusitis, upper respiratory infections, and laryngitis increased significantly during and in the days following the fires. For patients with a known respiratory condition, it is necessary to provide advanced warning so that they are better able to receive public health intervention and follow protocol necessary to avoid exacerbating the medical condition (Duclos et al. 1989). Improving the predictability of fires can correspond to an improvement on public health protocol for those with conditions which can be triggered or worsened by the inhalation of air polluted by fires.

While only 10% of all wildfires are caused by lightning, of the 20 largest fires recorded after 1932, eight were determined to be caused by lightning (CAL FIRE, 2018). Of these eight, two were located in Monterey County: the Basin Complex Fire, in June

2008, and the Marble Cone Fire, in July 1977 (CAL FIRE, 2018). These fires are unique as they were located in a coastal region, which Show and Kotok (1923) found is a less likely location for lightning-initiated fires than inland. The fires burned 162,818 and 177,866 acres, respectively.

Considering that lightning-initiated fires occur less frequently in coastal regions compared to inland regions, forecasting for coastal fire events is a comparatively difficult problem. The weather patterns contributing to the lightning-initiated fires in coastal regions are less understood due to the infrequency of coastal lightning events and the lack of comprehensive research studies of this event type. Most studies that discuss fires in California have focused on the distribution of fires throughout the state (Keeley 1982), as well as the effect fires pose to the ecosystem (Miller et al. 2012). While these studies provide useful information, from a meteorological standpoint, there is significant data missing, as the studies do not identify the specific weather events that caused the lighting.

van Wagtendonk and Cayan (2008) analyzed how lightning strikes vary temporally and spatially throughout California and noted that weather patterns were associated with lightning strikes. Specifically, the study found that the summer months contained the greatest number of lightning strikes, which correlated with localized high pressure in the western United States and increased moisture in regions south and east of California. Additionally, the study found that in the coastal bioregions the lightning strike density was below five strikes per year per 100 square kilometers. The study also calculated the number of lightning strikes for each bioregion in California between 1985 and 2000. The north and central coast regions received the least amount of total strikes during this time period with 15,530 and 18,264 strikes, respectively. However, for these coastal regions, the months of June, July, August, and September saw significantly more strikes than the other eight months. The summer month totals contributed to 77.8% of the north coast's total strike count and 80.4% of the central coast's total strike count. The study analyzed the 700 hPa geopotential height anomalies during the summer months, concluding that the increased number in lightning strikes in the north coast region corresponded with a negative anomaly to the south and a positive anomaly to the north. This pattern resulted in flow from south to east and corresponded with increased moisture levels over the north coast region (van

Wagtendonk and Cayan 2008). While this study provides useful insight into the temporal and spatial distribution of lightning strikes throughout California, it only indicates a general weather pattern, based on lightning events in the entirety of California, rather than a specific synoptic-scale pattern that generates lightning in coastal California.

Lightning activity during the cool season, winter and spring, in coastal California most likely occurs in the presence of landfilling storm systems, where cold air and steep lapse rates at mid-levels are introduced above the ocean-moderated maritime air mass at the surface. Additional research is needed to characterize the specific types of synoptic scale systems that contribute to cool season lightning events. During the warm season, summer and fall, coastal regions are generally characterized by low-level subsidence inversions (Iacobellis et al. 2009). Subsidence inversions are generated when there is "an increase in temperature with height that is produced by adiabatic warming of a layer of subsiding air," (American). In coastal regions of California, the cooler temperature of the Pacific keeps the surface temperature relatively cool. In the summer months, the air aloft is generally warmer, which contributes to the formation of an inversion when the warmer layer descends to meet to the cooler boundary layer (Iacobellis and Cayan 2013). Due to the inversion that dominates the coastal region of California during the summer months, convection and storms are limited (Elliot 1958). Typically, for coastal regions, researchers and forecasters believe that when storms occur, they are rooted in an elevated layer of conditional instability above the marine boundary layer, potentially due to anomalous southerly moisture transport in this layer. Since there are few studies that specifically characterize the summertime convective activity in coastal California, a comprehensive assessment of these events is needed, which motivates this research. The conditions for warm season storms are particularly of research and forecasting interest as, on average, coastal California receives very little rainfall during the warm season which increases the risk of fires in coastal California during this time.

The goal of this study is to categorize the typical synoptic scale conditions that bring lightning to coastal California during both the cool season and warm season months. Typically, convective available potential energy (CAPE) is required for the development of thunderstorms. Therefore, the properties of the synoptic scale patterns that generated

thunderstorms were assessed to understand what characteristics of the synoptic scale patterns favored the presence of CAPE over coastal California. It is hypothesized that the cool season and warm season months will be dominated by distinctly different flow patterns: the cool season being characterized by well-developed synoptic scale systems with strong flow and quasi-geostrophic forcing for ascent and surface-based CAPE and the warm season having predominately weak synoptic scale flow and ascent with elevated CAPE.

II. METHODS

The focus of this study was on the coastal region of California, defined by any point within 50 km of the shore of the state, including 50 km offshore. Lightning data were obtained from the National Center for Environmental Information (NCEI) Gridded summaries. This product compiles daily cloud-to-ground strike counts within 4 km by 4 km grid boxes centered on an Albers equal area 4 km grid. The data used to generate the NCEI lightning gridded product was obtained from the Vaisala Corporation's lightning detection network. An "event day" was defined as any day that a grid box centered within 50 km of the coast of California recorded a strike over the period from 2005 to 2011. The spatial centroid for each event day is the weighted average of different points based on the number of strikes per point. The spatial centroid is defined as

$$\vec{\boldsymbol{C}} = \frac{\sum_{i=0}^{N} \vec{\boldsymbol{x_i}} n_i}{\sum_{i=0}^{N} n_i}, \tag{1}$$

where N is the number of grid boxes within 50 km of the coast that recorded a strike on a given day, n_i is the number of strikes in the *i*th grid box on that day, $\vec{\boldsymbol{x_i}}$ is the *x* and *y* location of the *i*th grid box, and $\vec{\boldsymbol{C}}$ is the x and y strike centroid location on a given day. Atmospheric data were obtained from the NCEP Global Forecast System (GFS) single degree resolution global analysis (Juang 2014). Temperature, geopotential height, zonal wind, meridional wind, and relative humidity data were obtained on 21 vertical levels, 1000:900 mb at 25 mb increments and from 900:100 mb at 50 mb increments, for each event at 00 UTC, 06 UTC, 12 UTC, and 18 UTC within an 80 degree by 80 degree box centered at the event centroid point. The latitude of the box ranged from 32.17° to 42.23°. The longitude of the box ranged from 117.07° W to 124.7° W.

To determine if multiple distinctive synoptic scale patterns that led to coastal lightning events exist, principal component analysis (PCA) was applied to the atmospheric data following the methodology of Mercer et al. (2012) and Peters and Schumacher (2014). PCA is a statistical post-processing technique that compresses large datasets and efficiently indicates if the data falls into distinct clusters. The following method briefly details the computational steps necessary to apply PCA to our atmospheric data. For a more detailed

description of the methodology, see Wilks 2006). First, a 30 degree by 30 degree subset of the geopotential height data was selected from the center of the 80 degree by 80 degree boxes centered at the event centroid. The data was subset in order to focus on a smaller region, which made computations easier. *N*, *M*, and *K* correspond with the number of grid points in the X, Y, and vertical directions, respectively. *E* is the number of events, with atmospheric data compiled for four times per event day. The individual variables of the data were averaged over all events and times for each grid point. The average was then subtracted from the atmospheric data. Each grid point was normalized by the standard deviation at the respective point over all events and times. The geopotential height data were reshaped into $\vec{\boldsymbol{Z}}$, a two-dimensional matrix with dimensions Q by E, where $Q = N \times M \times K \times 4$. Qualitatively, *Q*, is the number of grid points per event. For every grid point there is one principal component (PC). Though other variables were not directly used in the PCA computation, they were used to construct composites later on to examine their structure for each principal component. Thus, *Q* is the corresponding number of principal components for the study. The correlation matrix $\vec{\boldsymbol{R}}$ of $\vec{\boldsymbol{Z}}$ was computed as

$$\vec{\boldsymbol{R}} = \frac{\mathbf{1}}{\boldsymbol{Q-1}}\vec{\boldsymbol{Z}}^{\boldsymbol{T}}\vec{\boldsymbol{Z}} \, . \tag{2}$$

The matrix $\vec{\boldsymbol{Z}}$ is expressed in terms of principal components (PCs) as

$$\vec{\boldsymbol{Z}} = \vec{\boldsymbol{F}}\vec{\boldsymbol{P}}^{\boldsymbol{T}} \, , \tag{3}$$

where $\vec{\boldsymbol{F}}$ is a *Q* x *E* matrix that contains the PCs and $\vec{\boldsymbol{P}}$ is an *E* x *E* matrix that contains the loading factors for each PC in each event. In order to solve for the loading factor, $\vec{\boldsymbol{P}}$, in Equation (3), two additional equations were required

$$\vec{\boldsymbol{R}} = \vec{\boldsymbol{E}}\vec{\boldsymbol{D}}\vec{\boldsymbol{E}}^{\boldsymbol{T}} \tag{4}$$

$$\vec{\boldsymbol{P}} = \vec{\boldsymbol{E}}\vec{\boldsymbol{D}}^{\mathbf{1}/\mathbf{2}} \, , \tag{5}$$

where $\vec{\boldsymbol{E}}$ is the eigenvector matrix of $\vec{\boldsymbol{R}}$, and $\vec{\boldsymbol{D}}$ is a diagonal matrix that contains the singular values that correspond to each eigenvector in $\vec{\boldsymbol{E}}$. The PCs were subsequently obtained by substituting $\vec{\boldsymbol{P}}$ into Equation (3) and solving for $\vec{\boldsymbol{F}}$. The Q PCs in $\vec{\boldsymbol{F}}$ are essentially maps

that show patterns of spatial variability. The loadings, $\vec{\boldsymbol{P}}$, quantitatively correspond with the magnitude and direction of the given event within that pattern of variability. Once the PCs were generated, they were sorted so that the leading PC is a pattern that corresponds with the largest pattern of variability in $\vec{\boldsymbol{Z}}$, the secondary PC corresponds with the second largest pattern of variability, etc. Therefore, applied to our study, the leading PC corresponds to the largest pattern of spatial variability among the lightning events. For example, a PC pattern may correspond with a local geopotential height anomaly. A large, positive loading on the PC would be characterized by geopotential height ridging and a jet stream that deviates northward over the region. A large, negative loading on the PC would be characterized by geopotential height troughing and a jet stream that deviates southward over the region. The loading factors highlight the degree of similarity between events. Large-in-magnitude loadings corresponds with a PC that more closely matches the original pattern, while small-in-magnitude loadings on a PC corresponds with a PC that less closely matches the original pattern. Thus, similar loadings indicate similar events and large differences in loadings indicate events that are very different from one another.

The three leading PCs of our dataset explained 21%, 6%, and 5% of the total variance of the dataset all remaining PCs explained less than 5% of the total variance. Therefore, the analysis was restricted to focus on parameterizing the loadings on the primary and secondary PCs, indicated henceforth as PC1 and PC2, respectively. PC1 and PC2 were selected because they explained a disproportionately large percentage of variance compared to other loadings (Figure 1).

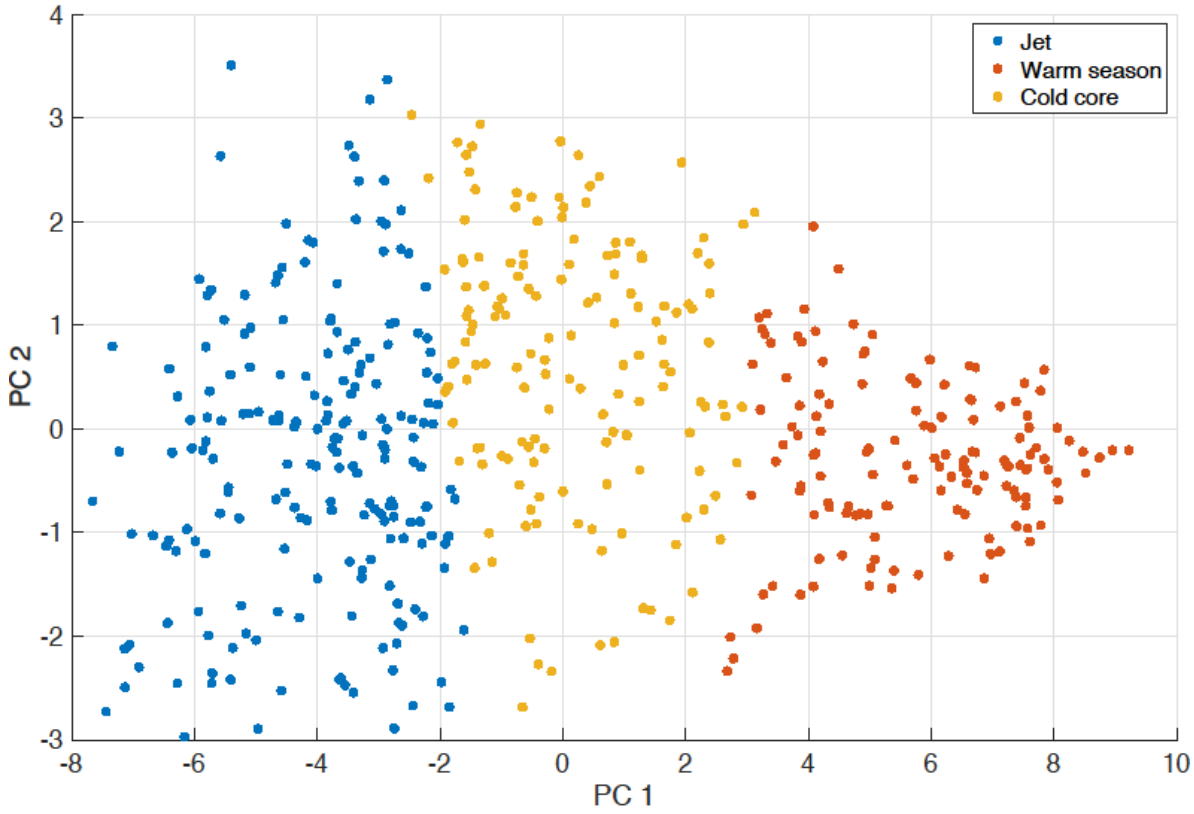

Figure 1. PC1 vs PC2 distribution showing the clustering of the jet-type (blue), warm-season (red), and cold-core low (yellow) event types.

Similar to Peters and Schumacher (2014), K-means cluster analysis was performed on the loadings of PC1 and PC2. K-means clustering allows the user to determine the number, n, of clusters the data contains with each point in the cluster being closest to that particular cluster's mean value, compared to the mean value of other clusters. We applied k-means clustering for n=2 through n=15, which determined that the best subjective distinction between event types occurred with n=3. Increasing the number of clusters greater than three produced multiple event type with subjectively similar characteristics, thus, n=3 is the largest number of clusters that achieves subjectively distinguishable clusters. These three distinguishable clusters correspond to our three distinguishable event types. Each of the three climatological patterns featured distinct lower tropospheric flow patterns and lower to middle tropospheric temperature trends. For the purpose of clearly

distinguishing each case, three naming conventions will be used. Case 1 will be referred to as “Jet-type;” case 2 will be referred to as “cold-core low;” case 3 will be referred to as “warm-season.”

Using radar imagery, random dates with lightning events where vetted to ensure that the data was accurately indicating the presence of lightning. From these dates, three were chosen, one for each event type, and the respective radar imagery, 300 mb synoptic patterns, and 500 mb synoptic patterns were plotted from the UCAR database (figures 2, 3, and 4). The jet-type event selected was November 20, 2011. The radar imagery indicates the presence of convection along the Northern California coast. The 300 mb and 500 mb synoptic patterns confirm the presence of an upper-level jet impacting the California coast, which we note later in the study is characteristic of our jet-type events (Figure 2). The cold-core low event selected was December 13, 2011. The radar imagery shows that convection occurred along the Southern California coastline. The 300 mb and 500 mb synoptic patterns confirm the presence of a mid-to-upper-level cutoff low that has moved down the California coast, which we note later in the study is characteristic of our cold-core low event type (Figure 3). The warm-season event selected was September 11, 2011. The radar imagery indicates convection along the Southern California coast. As noted later in the study, the 300 and 500 mb synoptic pattern for the event shows the characteristic warm season flow, a localized trough over California with a large-scale upper-level ridge arching over Canada (Figure 4).

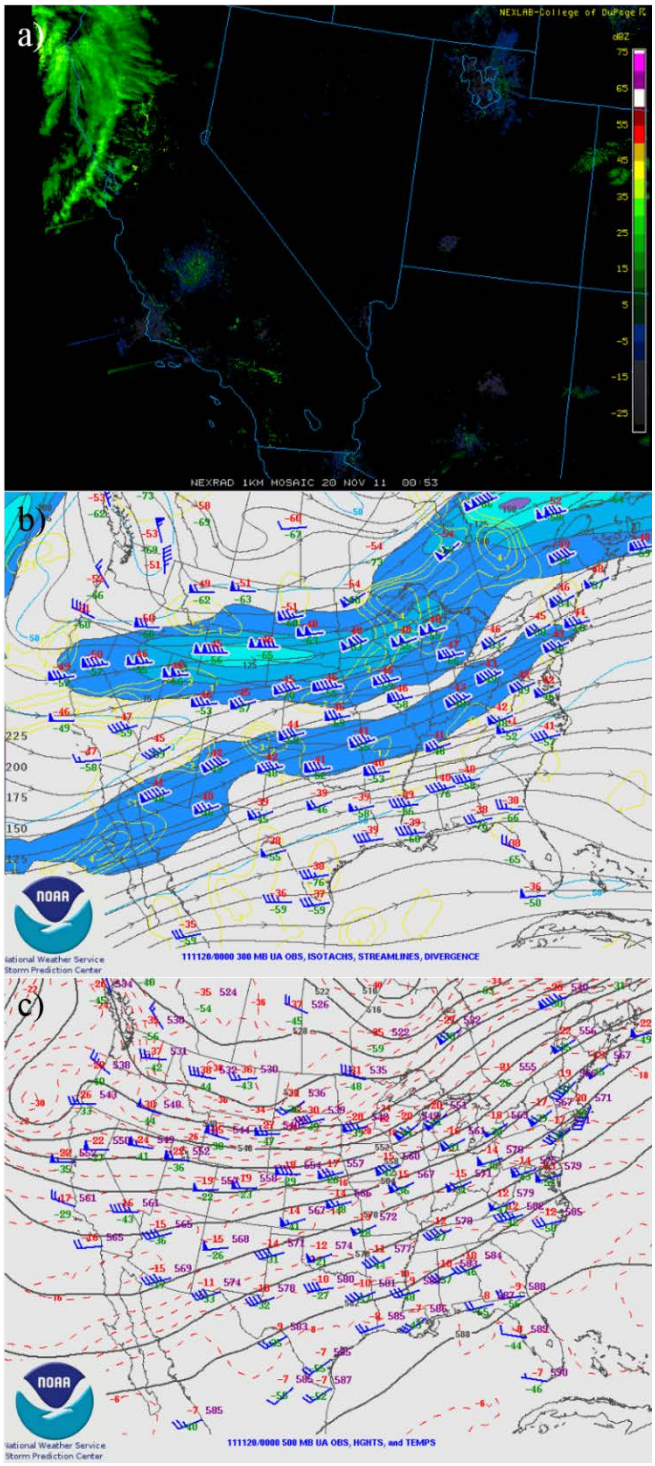

Figure 2. Jet-type event on November 20, 2011 with (a) radar, (b) 300 mb wind barbs (kt), streamlines (contours), divergence (shading), temp observations (°C); (c) 500 mb geopotential heights (contours), wind barbs (kt), temp observations (°C)

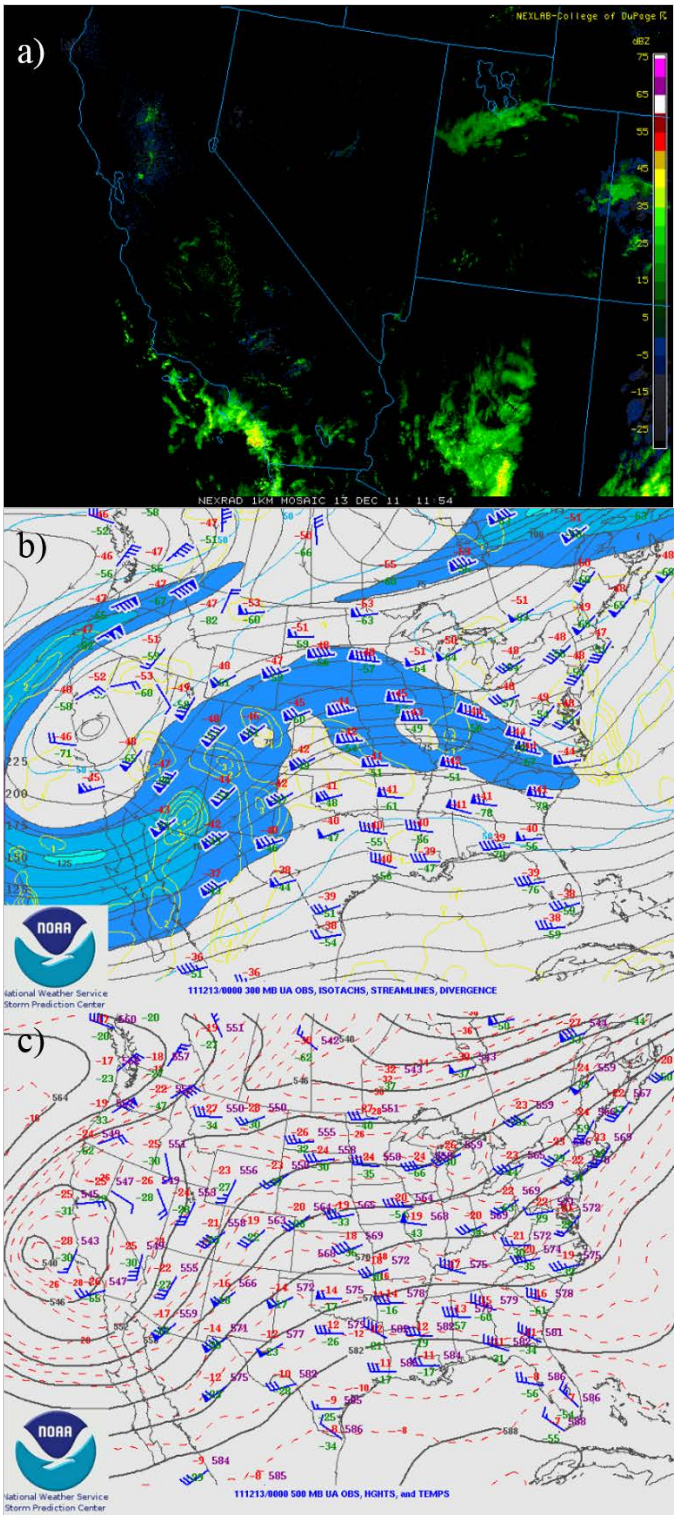

Figure 3. Cold-core low event on December 13, 2011 with (a) radar, (b) 300 mb wind barbs (kt), streamlines (contours), divergence (shading), temp observations (°C); (c) 500 mb geopotential heights (contours), wind barbs (kt), temp observations (°C)

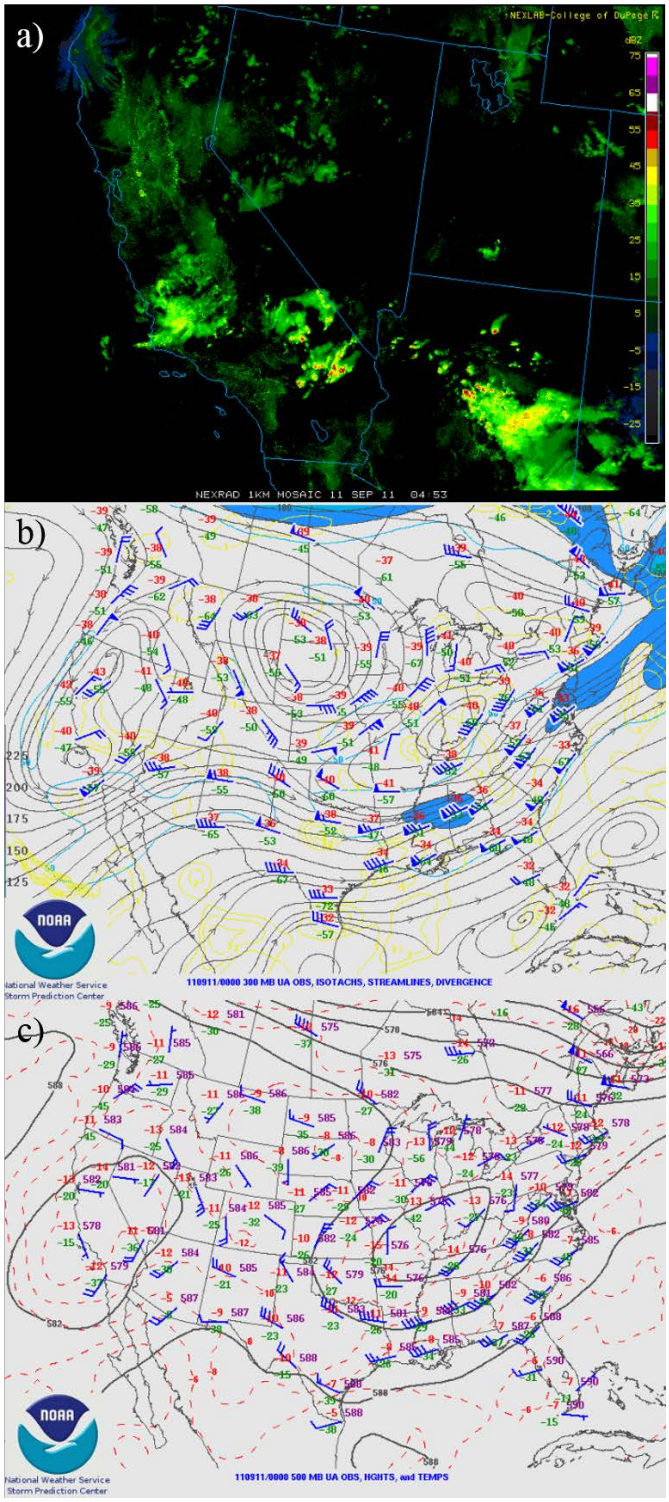

Figure 4. Warm-season event on September 11, 2011 with (a) radar, (b) 300 mb wind barbs (kt), streamlines (contours), divergence (shading), temp observations (°C); (c) 500 mb geopotential heights (contours), wind barbs (kt), temp observations (°C)

Once the number of event types was found, composites were generated using the NCEP GFS atmospheric dataset. For each event type, the atmospheric data for the event days that corresponded with each respective event type were compiled and averaged at the spatial centroid. Composites of the following fields were used to generally characterize the synoptic scale features associated with events: 300 hPa wind speed and geopotential height, 850 hPa temperature profile and geopotential height. Additionally, composites of 700–400 hPa lapse rate, 700 hPa relative humidity, and 700 hPa water vapor mixing ratio were examined in order to determine how the synoptic scale patterns associated with events contributed to the formation of CAPE. Anomalies of these CAPE related quantities were also examined, where the average of a given quantity for a given event over the 2005–2011 timeframe, and over the month of a given event was subtracted. Finally, composite profiles of CAPE and skew-T diagrams were compared among events. CAPE was computed for each event at the event centroid by lifting air parcels from each vertical level and integrating the air parcels' buoyancies, prior to constructing the composites.

THIS PAGE INTENTIONALLY LEFT BLANK

III. RESULTS

The data yielded three significant climatological patterns that occurred with lightning strikes in coastal California. Our study indicated that the winter months, December through March, had the highest cloud-to-ground lightning events, with March being the month with the greatest number of events (Figure 5). This data contradicts van Wagtendonk and Cayan's (2008) finding that the summer months had the greatest number of strikes in coastal California. It is possible that the difference is due to how our study defined the coastal region of California, as compared to how van Wagtendonk and Cayan (2008) defined the coastal bioregions. van Wagtendonk and Cayan (2008) referenced the map of ecological subsections of California found in Miles and Goudey (1997). The study defined the coastal region of California by ecosystem, not measurable distance from the coast. Therefore, it is evident that some of the area van Wagtendonk and Cayan (2008) categorized as coastal was not considered to be coastal in the context of our study, where we defined the coastal region of California to be within 50 km of the coast. Although, this is a notable difference in how our study differed from that of van Wagtendonk and Cayan (2008) it is possible that because our study was conducted over a smaller time frame, seven years, versus 16 years, that our results varied significantly. Further study should be conducted to rule out the use of less data as a limiting factor in the study.

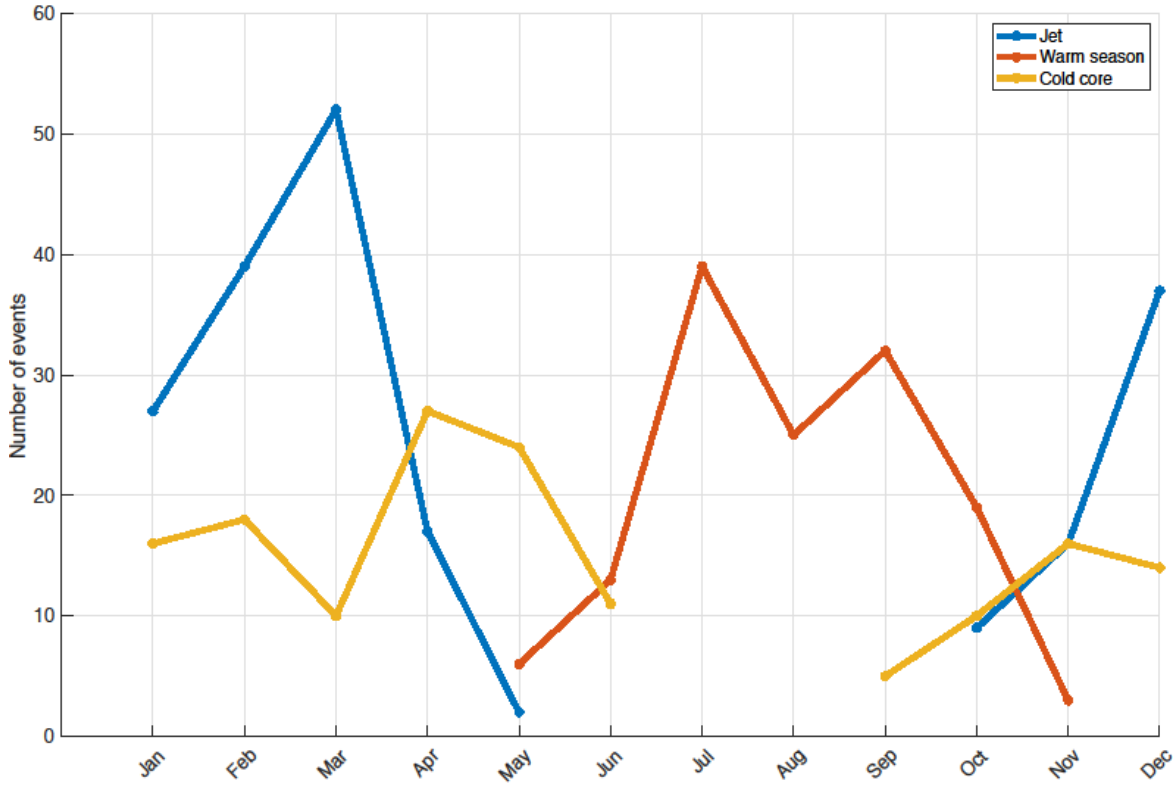

Figure 5. Distribution of events per month for the jet-type (blue), warm-season (red), and cold-core low (yellow) event types.

The jet-type case involves a strong upper-level jet impacting the west coast (Figure 6). In addition to the upper-level-jet, a strong onshore low-level jet was also found in this event type (Figure 7). Jet-type events typically occurred in the late winter and spring (Fig 5) and occurred with surface-based CAPE (Figure 8). The cold-core low case is characterized by either a strong trough or cutoff mid-to-upper-level low descending through California (Figure 6). This event typically occurs throughout the cold season months and, like the jet-type case, occurs with surface-based CAPE (Figure 8). The warm-season case is characterized by a large-scale upper-level ridge and a weak localized upper-level trough (Figure 6) and, as noted later in the paper, paired with moisture aloft and elevated CAPE in the atmosphere (Figure 8). As noted by the case name, this event occurs during the warm-season (Figure 5), June through October

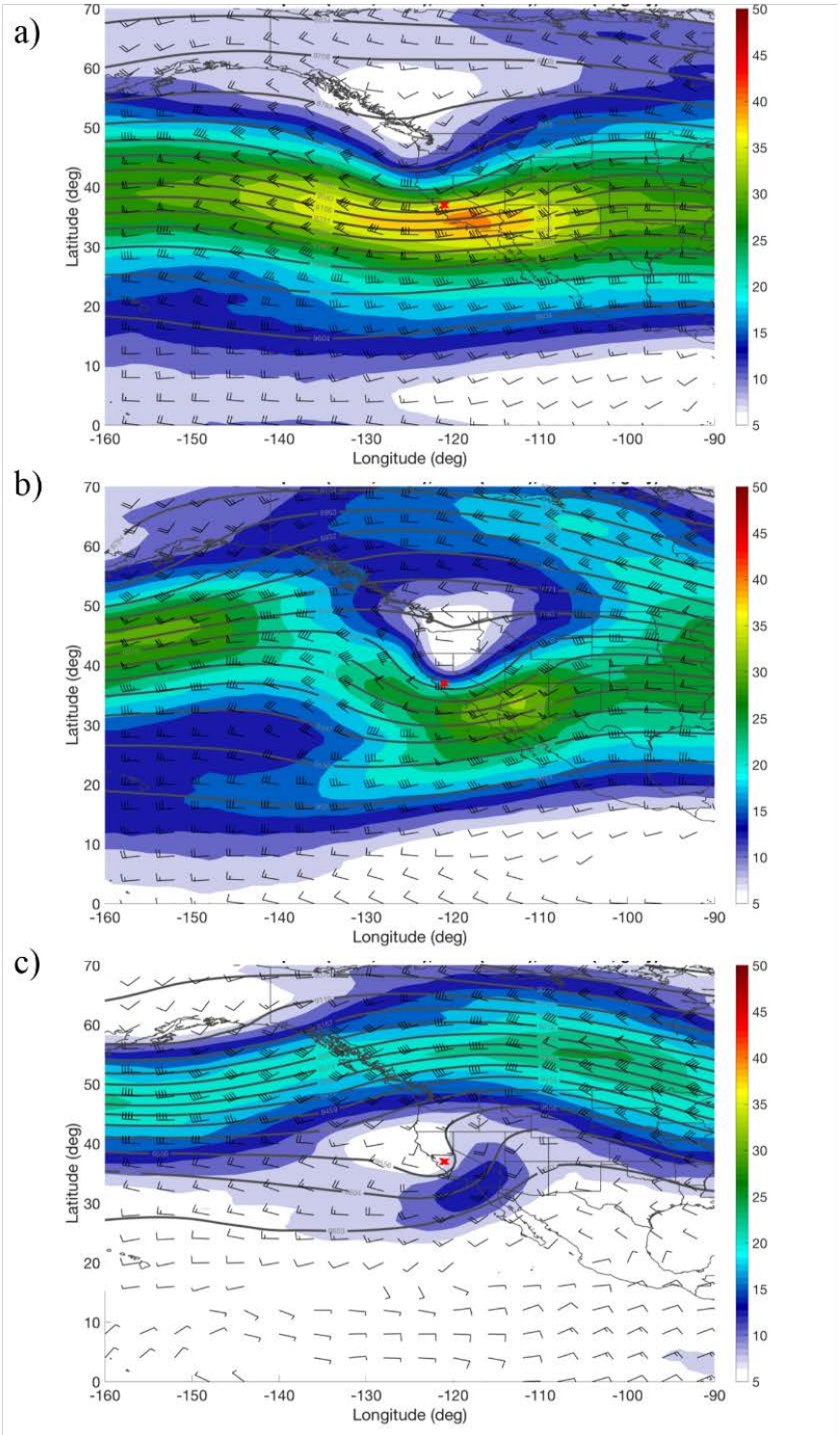

Figure 6. Composites of atmospheric fields at 300 hPa generated using 1800 UTC data from each event relative to the event center (red x). Wind speed (shading, m s^{-1}), wind barbs (kt), geopotential height (contours, m). (a) jet-type, (b) cold-core low, (c) warm-season

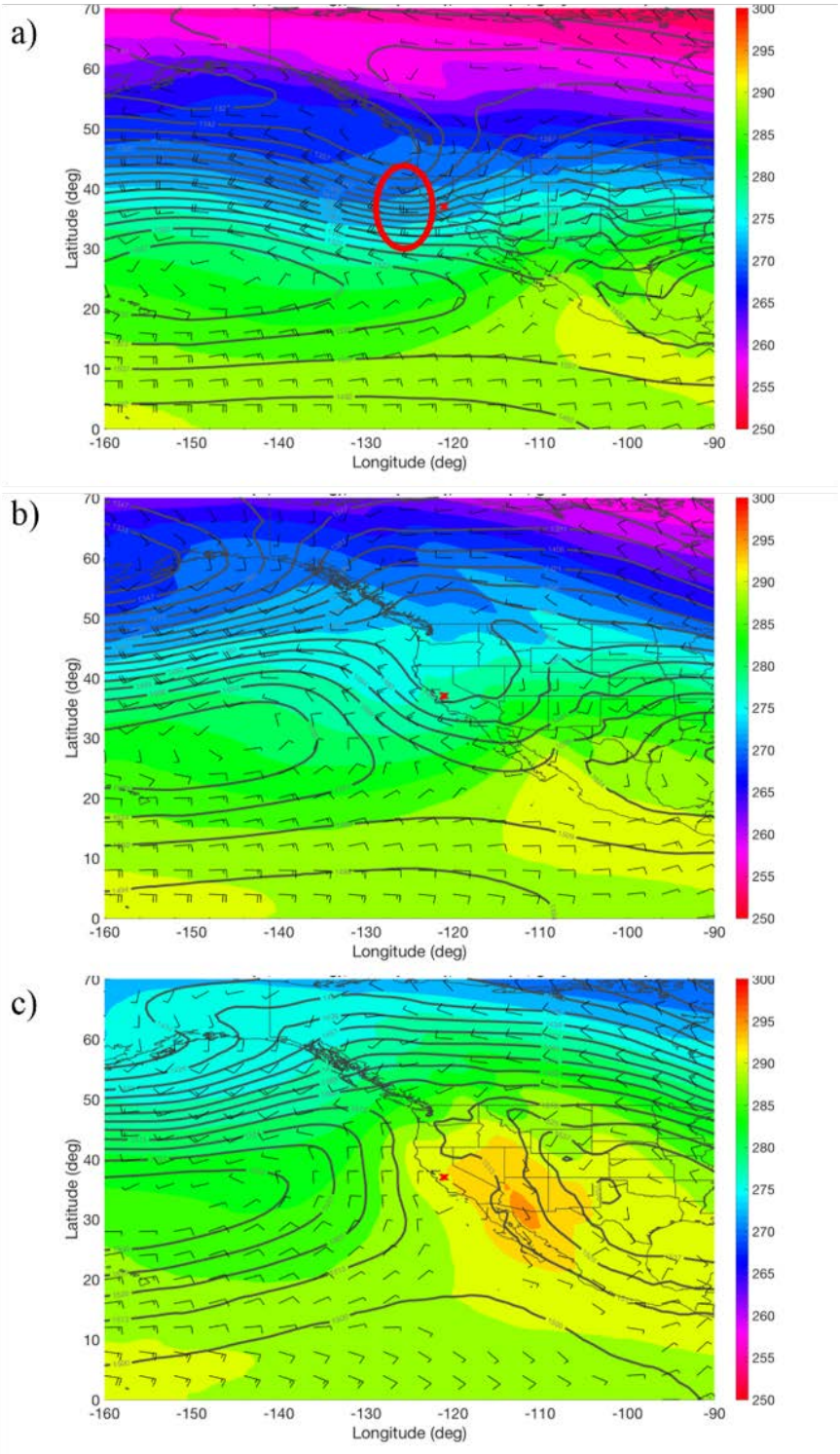

Figure 7. Composites of atmospheric fields at 850 hPa using 1800 UTC data for each event relative to the event center (red x). 850 hPa temperature (shading, K), wind barbs (kt), geopotential height (contours, m) (a) jet-type with low-level jet (red circle), (b) cold-core low, (c) warm-season

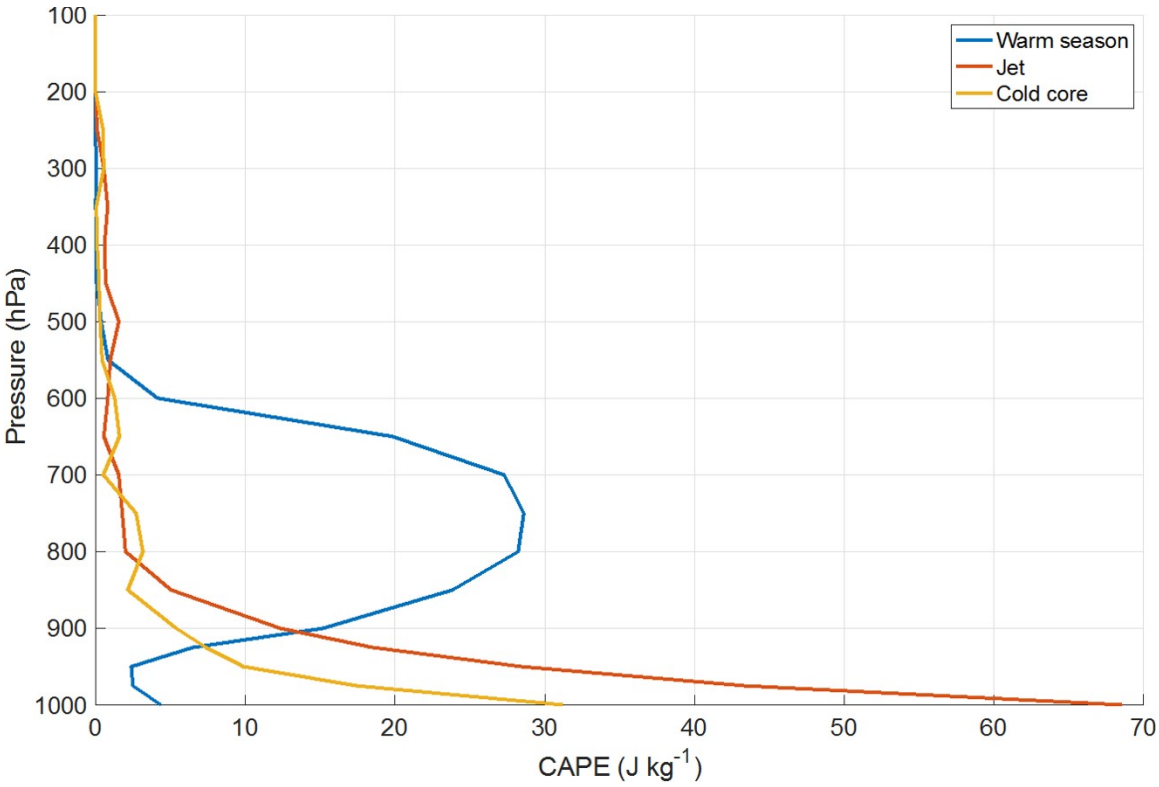

Figure 8. CAPE (J kg^{-1}) as a function of height (hPa) for the warm-season (blue), jet-type (red), and cold-core low (yellow) event types.

Upper-level dynamics, as shown in Figure 6, indicate the presence of different features for the three case types. The composites were centered at the geographic center of all of the events, as noted by the red x. The jet-type case is characterized by a strong upper-level jet streak that impacts the coast of California (Figure 6). The cold-core low case type shows strong upper-level flow to the south of the event center (Figure 6). In this case the event center is underneath an upper-level trough. The event center in the warm-season event type is substantially further south of the upper-level jet than the cold-core and jet event types (Figure 6). In this case, the event center is associated with a weak trough and a large-scale ridges with southwesterly flow aloft (Figure 6).

The 850 hPa temperature shows that each event type has a unique low-level flow and temperature distribution (Figure 7). For the jet-type events, a strong low-level jet impacts the coast with winds up to 25 knots, as indicated by the red circle on Figure 7. Due to the strong low-level onshore flow in these events, strong orographic lift may have

accompanied the baroclinic processes and facilitated the initiation and organization of convection, though an in-depth mesoscale analysis would be needed to confirm this suspicion. Additionally, the jet-type events have flow that is parallel to the temperature contours (Figure 7), while the cold-core low event has flow more perpendicular to the temperature contours (Figure 7). The cold-core low event has strong CAA to the left of the event center with northwesterly flow parallel to the coast (Figure 7). This CAA indicates southward frontal passage. The warm-season event profile indicates the presence of weak offshore flow at the lower levels (Figure 7) and weak temperature advection, with no discernable fronts present.

CAPE, which is an essential element for convection, is determine by low level temperature and moisture and mid-to-upper-level lapse rates. Steeper lapse rates typically correspond with more CAPE due to cold air aloft sitting above warmer air below, causing instability. The 700–400 hPa temperature difference (defined as T_{400}–T_{700}, where the temperatures correspond to the 400 hPa and 700 hPa, respectively) was used to determine the mid-to-upper level lapse rate for each of the individual event types. The 700–400 hPa temperature profile (Figure 9) indicates the presence of a negative anomaly in all three event types, showing that mid-level lapse rates were anomalously steep during the lightning events. These steep lapse rates were facilitated by the presence of anomalously cold air aloft in the cold-core and jet event types, and by the presence of anomalously cool air at upper levels and warm air at low levels in the warm-season event types. Additionally, the vertical temperature profiles showed that all event types had cooler than average temperatures throughout the atmosphere (Figure10). However, by analysis of Figure 10, it is evident that the jet-type and cold-core low events had the coolest anomalies in the middle troposphere, while the warm-season events had slightly anomalously cooler temperatures at mid-levels than they did at low-levels. Thus, all three event types favor anomalously large CAPE because of their anomalously steep lapse rates, which is what would be expected for weather patterns that correspond with lightning events.

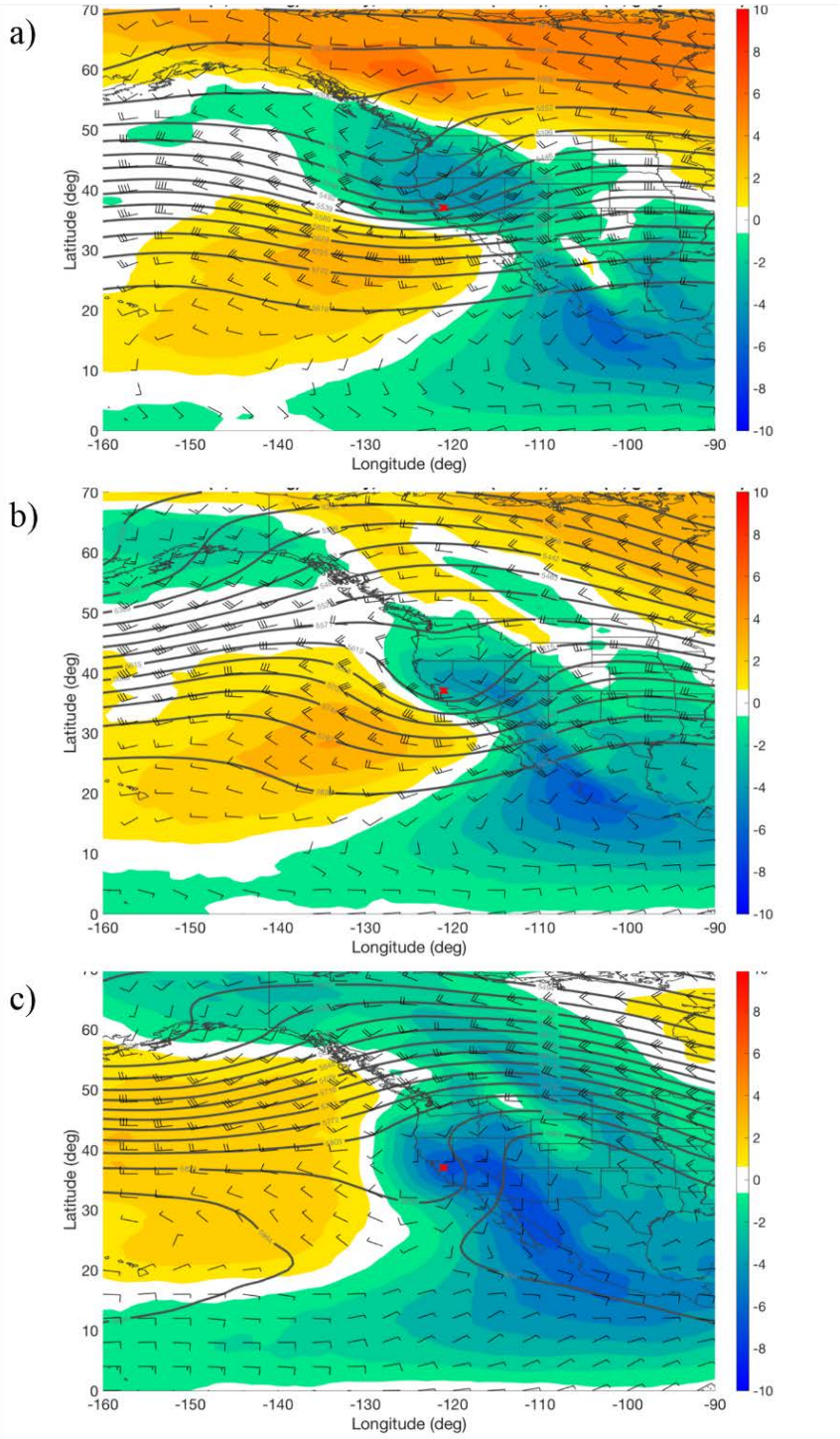

Figure 9. Composites centered at the event center (red x) of atmospheric fields showing 700-400 hPa temperature difference (shading anomaly, K), 900 hPa wind (barbs), and geopotential height (contours, m) (a) jet-type, (b) cold-core low, (c) warm-season

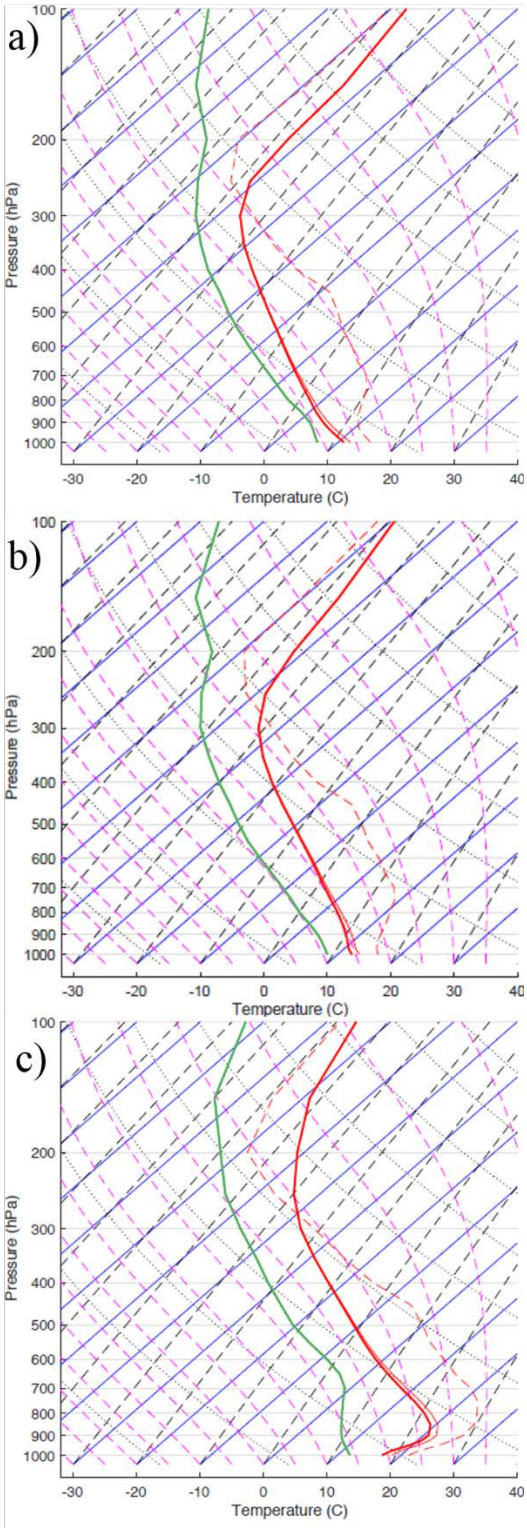

Figure 10. Vertical profile comparing composite temperatures to climatological monthly mean temperature (dashed red line) for (a) jet-type, (b) cold-core low, (c) warm-season events.

Additionally, the warm-season event type shows the steepest lapse rates for mid-to-upper-levels, as compared to the cold-core low and jet event types. This indicates that the warm-season has the greatest potential for instability, compared to the other case types, which occur more prominently during the fall, winter, and spring. This finding is contradictory to our results that more lightning strikes occur in the winter through early spring. However, van Wagtendonk and Cayan (2008) found that the summer months feature a prominent increase in lightning strikes compared to the winter months. This contradiction in our results warrants further study with a larger data set to confirm that the temporal distribution of strikes is accurate over a longer time period.

The temperature and CAPE profiles indicate the original vertical position of the air parcels with the most CAPE. As discussed previously, CAPE is surface-based in jet-type and cold-core low events, while CAPE is elevated in warm-season events (Figure 8). The CAPE profiles show CAPE for parcels lifted from each level (Figure 8). For instance, CAPE at 800 mb represents the CAPE for an air parcel lifted from 800 mb. Additionally, the vertical profiles indicate whether or not the event types correlate with inversions. The jet-type and cold-core low events do not typically occur with low-level inversions (Figure 11), while the warm-season event type is connected with a low-level temperature inversion (Figure 11). The presence of a low-level inversion and elevated CAPE in the warm season event types indicates that storms in these events derive their energy from the layer of air above the marine boundary layer, and likely correspond to elevated, rather than surface-based, convection.

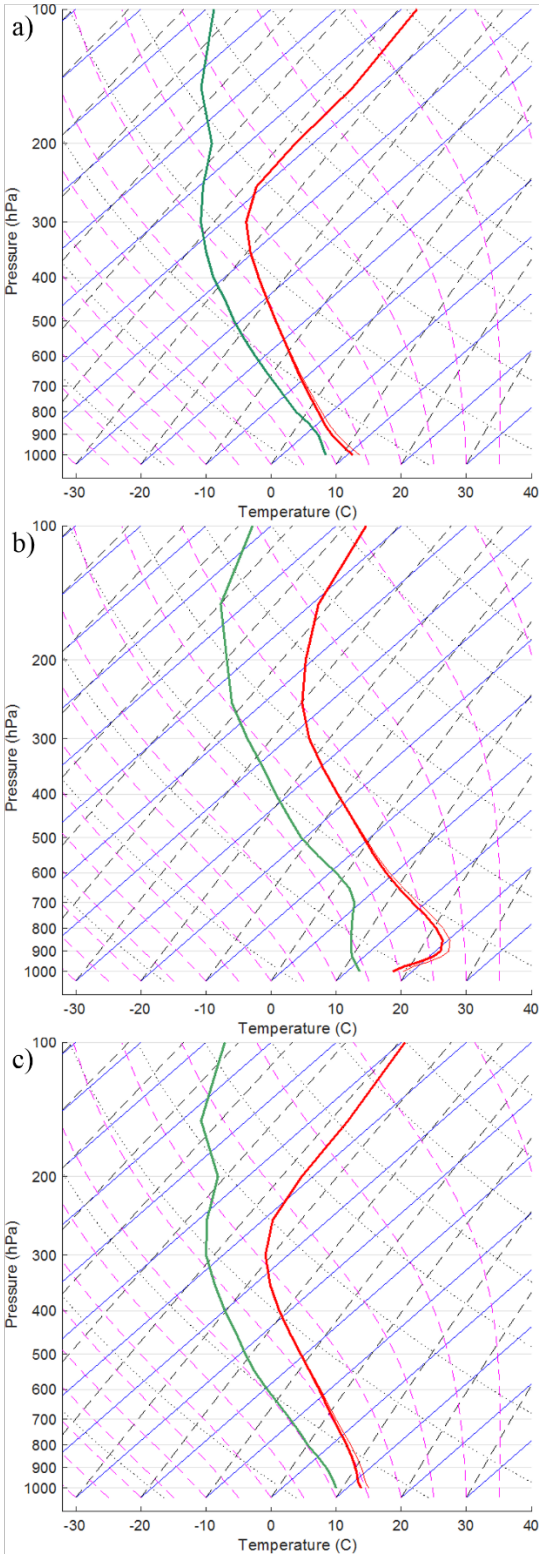

Figure 11. Average vertical profile for each event type. (a) jet-type, (b) cold-core low, (c) warm-season

For the warm-season event types, CAPE is maximized at 700 hPa (Figure 8). The moisture at the level the parcel is lifted from has a significant impact on CAPE. Therefore, the 700 hPa relative humidity anomaly (Figure 12) and the 700 hPa water vapor mixing ratio anomaly (Figure 12) were analyzed. The 700 hPa relative humidity anomaly was used to indicate whether the atmosphere was more or less humid than normal during warm-season lightning events. The 700 hPa water vapor mixing ratio anomaly, was used to indicate whether the atmosphere contained more or less water vapor than normal during warm-season lightning events. Both the relative humidity and water vapor mixing ratio anomalies indicate that during warm-season lightning events, southerly flow brings anomalous moisture into the region. Coupled with the presence of steep mid-level lapse rates, indicated by the 700–400 temperature difference profile (Figure 9), there are multiple factors that indicate that the CAPE is strengthened relative to its climatological value during the warm-season events.

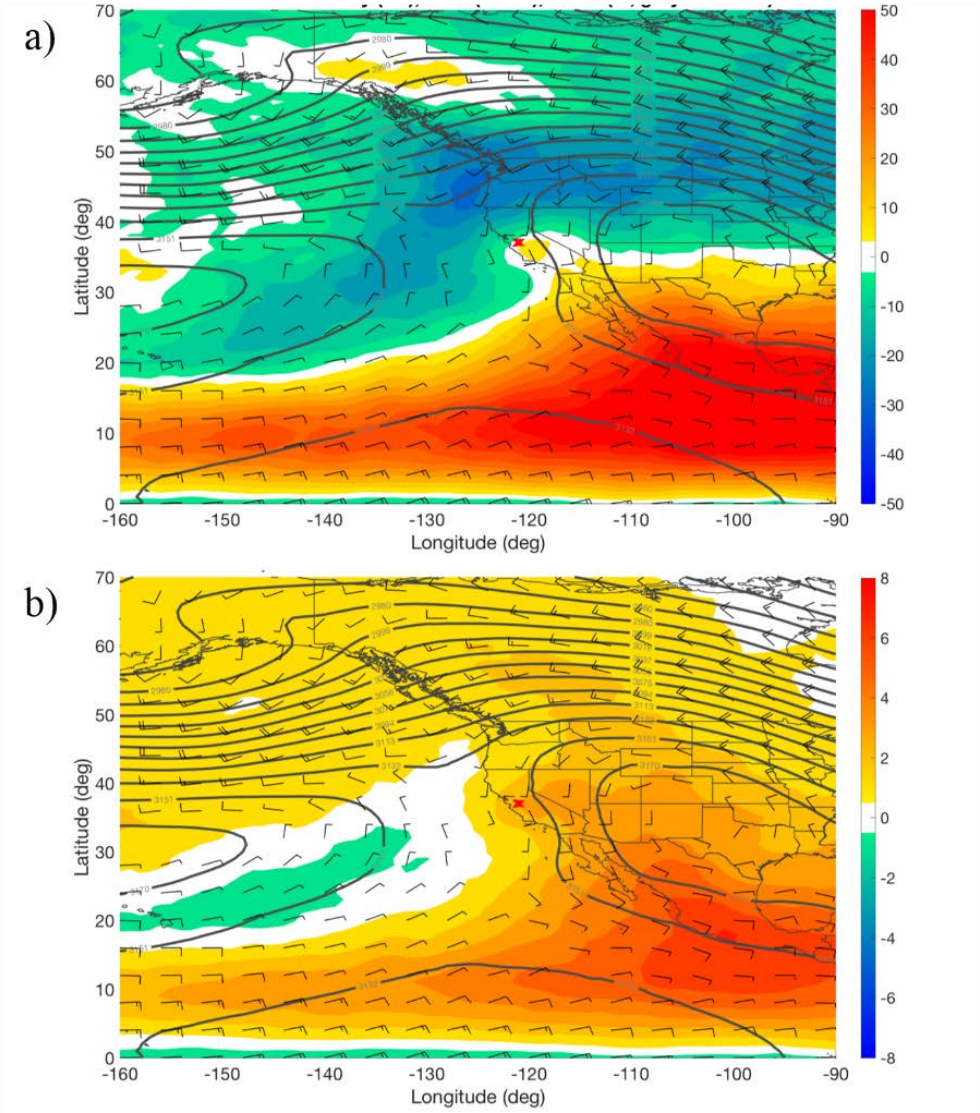

Figure 12. Composites of warm season event atmospheric distributions centered at the event center (red x) for (a) 700 hPa relative humidity anomaly (%) with wind barbs (kt) and geopotential heights (contours, m) and (b) 700 hPa mixing ratio anomaly (g kg^{-1}) with wind barbs (kt) and geopotential heights (contours, m)

IV. DISCUSSION AND CONCLUSION

Forecasting for warm-season lightning event types is a critically important problem. As shown by the data, the warm-season events are characterized by increased levels of relative humidity and water vapor in the atmosphere. Additionally, the warm-season events are most likely triggered by elevated CAPE. California is relatively dry throughout the summer months. Therefore, if cloud-to-ground lightning strikes do occur, there is an increased risk of wildfires. Due to the structure of the warm-season events, there is a possibility of lightning events that occur without rainfall. The skew-t for the warm-season (Figure 11) has a well-defined dry layer below the height of maximum CAPE which confirms the potential for dry thunderstorms, where precipitation evaporates in the dry layer before reaching the surface. This forecast scenario is markedly different than storms that occur towards the Sierras, which are typically paired with rainfall. The increased potential for dry thunderstorms during the summer months, when California is more than likely in dry conditions, poses a significant threat to environment and those who inhabit the region.

The warm-season event types also differ from the cold-core low and jet-type events due to the type of convection. Cold-core low and jet-type events are triggered primarily by surface-based CAPE, while warm-season event types are triggered by elevated CAPE. This leads to an increased challenge when forecasting for the warm-season events. Elevated CAPE is convection due to parcels of air that do not originate at the surface, which makes it potentially difficult to determine the source of the parcels that result in the warm-season event types (Peters et al. 2017). This difficulty results from the presence of many surface observations, but few upper-air observations, which leads to a greater potential for elevated CAPE layers to be inaccurately analyzed or missed completely (e.g., Peters et al. 2017). Additionally, the study by van Wagtendonk and Cayan (2008) found that coastal California received more lightning strikes during the summer months. Our research confirms that this is primarily due to the elevated CAPE that characterizes lightning events during the summer. However, our research differed from that of van Wagtendonk and Cayan (2008) in that, during the course of the study, we found that the winter and early spring months

were associated with a greater number of lightning strikes than that of the summer months. As noted previously, it would be beneficial to run our study over a longer time period in order to determine if the temporal distribution of lightning events is accurate. During the cold season, forecasters should pay particular attention to events that bring steep mid-level lapse rates into the region.

As noted above, the findings of our study indicated that cloud-to-ground lightning was more likely to occur during the winter season, November through March, with March having the largest number of lightning events (Figure 5). This result is similar to that found in Blier and Battan (1994). Their study found that roughly 80% of all tornadoes in California originated during the winter months of November through April, with the greatest number of events occurring in March. Additionally, the study found that the region with the greatest number of tornadic events was the southern California coastal region. While this study focused on tornadic activity and included the entire state of California, the parallel in results is not unusual. Tornadoes, like thunderstorms, require convection to occur (Blier and Battan 1994). Therefore, it would be expected that if the winter months had a greater number of strikes as compared to the summer months, the propensity for tornadoes would also be greater in the winter months than the summer months.

Additionally, a study that looked at synoptic patterns for different severe weather cases found synoptic patterns within the case studies that were similar to the three distinct event types indicated in our study (Neyman 2013). Specifically, the case study for the severe weather event on January 19, 2010, was synoptically characterized by the presence of an upper-level cold-core low with a strong jet at 300 mb (Neyman 2013). This event most likely was a cold-core low event type. The case study for the severe weather event on September 10, 2011, which features severe thunderstorms throughout southern California, closely aligns with our findings for warm season events. This storm was characterized by localized upper-level troughing over the western United States, weak offshore flow at 850 mb, and elevated convection. The elevated convection in this case occurred above an extremely stable boundary layer (Neyman 2013). Additionally, the event had notably steep lapse rates as well as high moisture advection at 700 mb (Neyman 2013), which our study found to be characteristic of the warm-season event type. A slight difference in our general

warm-season event type and this example case is that our warm-season event types were characterized by a large-scale upper-level ridge and a weak localized upper-level trough. Neyman only addresses the upper-level trough present in her selected study, so it would be assumed that no upper-level large-scale ridge was present in this scenario.

Monteverdi et al. (2003) found that tornadic convection typically occurs during the winter and spring months in California. The warm-season is generally characterized by presence of a capping inversion with a stable layer. This inversion, shown in our warm-season case vertical profile (Figure 10), inhibits the formation of deep convection. However, this inversion is not present during the event types that typically occur during the winter and spring, the jet and cold-core low cases. The vertical profile from our study for both the jet and cold-core low cases confirm that there is no low-level inversion that would prevent deep convection from occurring (Figure 10).

Overall, the primary findings of our research indicate the following:

- The warm-season event type is characterized by elevated CAPE, while the cold-core low and jet-type events are derived from surface-based CAPE.
- All event types favor anomalously steep mid-level lapse rates.
- Warm-season event types occur with southerly flow in the 800-600 hPa layer that brings anomalous moisture inland into southern California.
- The warm-season event type indicates the presence of a dry layer below 750 hPa which increases the potential for dry thunderstorms during the summer months.
- All lightning events correspond with steep mid-tropospheric lapse rates, indicating increased instability which favors larger CAPE

There are a few areas that require further study. First, as noted earlier in the paper, this study could be implemented over a significantly longer date range, to verify that the

findings hold true over a longer time period. Second, this scope of this study could be expanded to include inland regions of California, to determine if the synoptic conditions associated with coastal cloud-to-ground lightning events are similar to those conditions that contribute to lightning events that are more inland. Third, the findings in this paper could be applied to case studies of major lightning events in coastal California, to indicate if the research significantly improved the forecasting ability for these events.

Overall, this study provides information that will enhance the forecasting ability for lightning events in coastal California. Notably, there are two main areas that forecasters should pay attention to when forecasting for lightning events. First, the results indicate that forecasters need to pay attention to the specific forecast parameters that indicate potential for convection. The main parameter this study indicated was steep mid-level lapse rates are present in all three synoptic event types that occur with cloud-to-ground lightning. Next, the study found that the CAPE for all events was small, meaning it has the potential to not be analyzed in forecast models, which can lead to large errors in CAPE (Peters et al. 2017). Therefore, forecasters should pay attention to lapse rates as well as not discounting small CAPE values when forecasting for these types of events.

LIST OF REFERENCES

American Meteorological Society, American Meteorological Society: glossary of meteorology. [Available online at http://glossary.ametsoc.org/wiki/Subsidence_inversion].

Blier, W., K. A. Batten, 1994: On the Incidence of Tornadoes in California. *Wea. Forecasting*, **9**, 301–315.

CAL FIRE, 2009: Lightning Fires Within CAL FIRE's Jurisdiction. [Available online at http://www.fire.ca.gov/communications/downloads/fact_sheets/Lightning.pdf].

CAL FIRE, 2018: Top 20 Largest California Wildfires. [Available online at https://www.fire.ca.gov/communications/downloads/fact_sheets/Top20_Acres.pdf].

Duclos, P., L. M. Sanderson, and M. Lipsett, 1990: The 1987 Forest Fire Disaster in California: Assessment of Emergency Room Visits. *Archives of Environmental Health: An International Journal*, **45**, 53–58, doi:10.1080/00039896.1990.9935925.

Elliott, R. D., 1958: California storm characteristics and weather modification. *J.Meteorol.*, **15**, 486–493.

Iacobellis, S. F., and R. C. Daniel, 2013: The variability of California summertime marine stratus: Impacts on surface air temperatures. *Journal of Geophysical Research Atmospheres*, **118**, 9105–9122.

Iacobellis, S. F., J. R. Norris, M. Kanamitsu, M. Tyree, and D. R. Cayan, 2009: Climate variability and California low-level temperature inversions. CEC-500-2009-020-F, 62 pp, https://www.energy.ca.gov/2009publications/CEC-500-2009-020/CEC-500-2009-020-F.PDF.

Juang, H.-M. H., 2014: A discretization of deep-atmospheric nonhydrostatic dynamics on generalized hybrid vertical coordinates for NCEP global spectral model. NCEP Office Note 477, 40pp.

Keeley, J., 1982: Distribution of lightning and man-caused fires in California. *Proc. Proceedings of the Symposium on Dynamics and Management of Mediterranean-Type Ecosystems.* USDA Forest Service, PSW-58, Pacific Southwest Forest and Range Experiment Station, Berkeley, 431–43

Mercer, A. E., C. M. Shafer, C. A. Doswell III, L. M. Leslie, and M. B. Richman, 2012: Synoptic composites of tornadic and nontornadic outbreaks. *Mon.Weather Rev.*, **140**, 2590–2608.

Miles, S. R., C. B. Goudey.1997. *Ecological subregions of California: section and subsection descriptions.* USDA Forest Service, Pacific Southwest Region, San Francisco, California, USA.

Miller, J. D., C. N. Skinner, H. D. Safford, E. E. Knapp, and C. M. Ramirez, 2012: Trends and causes of severity, size, and number of fires in northwestern California, USA. *Ecological Applications,* **22**, 184–203, doi:10.1890/10-2108.1.

Monteverdi, J. P., C. A. Doswell, and G. S. Lipari, 2003: Shear Parameter Thresholds for Forecasting Tornadic Thunderstorms in Northern and Central California. *Weather and Forecasting,* **18**, 357-370

Neyman, I., 2013: Forecasting California thunderstorms, California State University, Northridge.

Peters, J. M., R. S. Schumacher, 2014: Objective categorization of heavy-rain-producing MCS synoptic types by rotated principal component analysis. *Mon.Weather Rev.*, **142**, 1716–1737.

Peters, J. M., E. R. Nielsen, M. D. Parker, S. M. Hitchcock, and R. S. Schumacher, 2017: The Impact of Low-Level Moisture Errors on Model Forecasts of an MCS Observed during PECAN. *Mon. Weather. Rev.*, **145**, 3599–3624

Show, S. B., E. I. Kotok, 1923: *Forest fires in California, 1911–1920: An Analytical Study.* U.S. Department of Agriculture, 88pp.

Smith, S. J., R. S. Anderson, 1992: Late Wisconsin paleoecologic record from Swamp Lake, Yosemite National Park, California. *Quatern.Res.,* **38**, 91–102.

van Wagtendonk, J. W., and D. R. Cayan, 2008: Temporal and spatial distribution of lightning strikes in California in relation to large-scale weather patterns. *Fire Ecology,* **4**, 34–56.

Wilks, S. D. 2006: *Statistical Methods in the Atmospheric Sciences.* Academic Press, 627 pp.

INITIAL DISTRIBUTION LIST

1. Defense Technical Information Center
   Ft. Belvoir, Virginia

2. Dudley Knox Library
   Naval Postgraduate School
   Monterey, California